R. Maneiro-Catoira, J. C. Brégains, J. A. García-Naya and L. Castedo, "Enhanced Time-Modulated Arrays for Harmonic Beamforming," in *IEEE Journal of Selected Topics in Signal Processing*, vol. 11, no. 2, pp. 259-270, March 2017, doi: 10.1109/JSTSP.2016.2627178.

Link to published version: https://doi.org/10.1109/JSTSP.2016.2627178.

Enhanced Time-Modulated Arrays for Harmonic Beamforming

Roberto Maneiro-Catoira, *Student Member, IEEE,* Julio Brégains, *Senior Member, IEEE,* José A. García-Naya*, *Member, IEEE,* and Luis Castedo, *Senior Member, IEEE*

***Abstract*—One of the primary features of time-modulated arrays (TMAs) is their ability to adapt their harmonic patterns to exploit the angular diversity of multipath wireless channels. In such a case, the TMA excitations must provide an adequate level of harmonic windowing in order to safeguard both the antenna efficiency and the signal-to-noise ratio (SNR) at reception. In this work, we propose to time-modulate the array excitations with periodic sum-of-weighted-cosine (SWC) pulses rather than with the periodic rectangular pulses corresponding to the on-off switches of conventional TMAs. We show how the larger flexibility of the SWC pulses allows for a more versatile design of the TMA harmonic radiation patterns without penalizing the array gain for each exploited harmonic.**

I. Introduction

SPATIAL diversity in wireless communications is usually exploited by means of antenna arrays and adaptive beamforming techniques. The radiation pattern of a linear antenna array can be adapted by periodically enabling and disabling the excitations of the individual array elements [1]. Such a technique is known in the literature as time modulation and can be easily implemented using hardware switches (see left-hand side of Fig. 1). From a signal processing perspective, time-modulated array (TMA) beamforming is a nonlinear operation that creates several radiation patterns at the harmonic frequencies of the periodic excitations. By properly adapting such harmonic patterns to the wireless channel, and by combining its corresponding outputs, TMAs are able to perform adaptive beamforming with the benefit of using a single radio frequency (RF) front-end [2], [3].

The on-off switching of the antenna array excitations involved in the TMA beamforming process is mathematically modeled as the multiplication between the antenna array excitations and periodic rectangular pulses [4], [5] (see right-hand side of Fig. 1). The frequency behavior of the rectangular pulses, however, is not the best one to efficiently distribute the spectral energy among the harmonic patterns to be exploited. Specifically, a minimum main-lobe width and a modest side-lobe level (SLL), together with a slow asymptotic side-lobe decay, are well-known characteristics of the rectangular pulses frequency response which will restrict not only the TMA efficiency but also the signal-to-noise ratio (SNR) level at the receiver. Hence, a pulse with a certain trade-off between its time and frequency responses is preferred for TMA beamforming. On the one hand, we seek for simplicity in the time domain in the sense that pulses would be easily generated. On the other hand, we look for pulses with some specific windowing features in the frequency domain.

As a first approach, and inspired by the so-called apodization procedures in signal processing[1], we look for suitable pulse functions which smoothly decay towards zero in the time domain with the aim of achieving a better performance in terms of SLL and asymptotic decay in the frequency domain. One possibility is the multiplication of a rectangular pulse by a sinusoidal function in the time domain. Such a multiplication causes a pulse shift in the frequency domain. Consequently, if a strategic linear combination of sinusoids (cosines) is used to multiply a rectangular pulse, a frequency response made up of a linear combination of weighted and frequency-shifted replicas of sinc functions will be obtained. This flexible way of smoothing the time response implies, of course, an increase of the pulse bandwidth (which is welcome when the objective consists in exploiting higher order harmonics) while providing room for shaping the frequency response.

With the previous ideas in mind, we find that the so-called sum-of-weighted-cosine (SWC) pulses [6], [7] are particularly adequate for our purposes, since they are precisely composed of frequency-shifted replicas of the sinc function, as illustrated in Fig. 3. Despite their simple form, such pulses allow for a flexible windowing of the harmonics involved. In addition to that, they provide an extra degree of freedom for the TMA harmonic patterns design. Hence, we have the following parameters to perform TMA beamforming:

- the usual TMA timing parameters, i.e, durations and shifts of the pulses, and
- a set of non-timing parameters corresponding to the weights of the SWC pulses.

Adaptive beamforming can be performed by changing dynamically the normalized time shifts and the SWC weights, while using statically the pulse time durations to design a quiescent (non-adapted) pencil beam pattern in the fundamental

* Corresponding author: José A. García Naya, jagarcia@udc.es.

The authors would like to express their gratitude to Dr. Lorenzo Poli and to Dr. Paolo Rocca (ELEDIA Research Center, University of Trento, Italy) for their support with the adaptive nulling algorithms.

This work has been funded by Xunta de Galicia, MINECO of Spain, and FEDER funds of the EU under grants 2012/287 and TEC2013-47141-C4-1-R.

R. Maneiro-Catoira, J. Brégains, J.A. García-Naya, and L. Castedo are with the Universidade da Coruña (University of A Coruña), A Coruña, Spain.

Email: {roberto.maneiro, julio.bregains, jagarcia, luis}@udc.es.

Digital Object Identifier

[1] In discrete-time signal processing the samples may be abruptly truncated causing unwanted frequency side-lobes when performing the discrete Fourier transform. Such an abrupt truncation can be smoothed by properly multiplying the corresponding sample region times a suitable time function. This procedure is known as apodization.

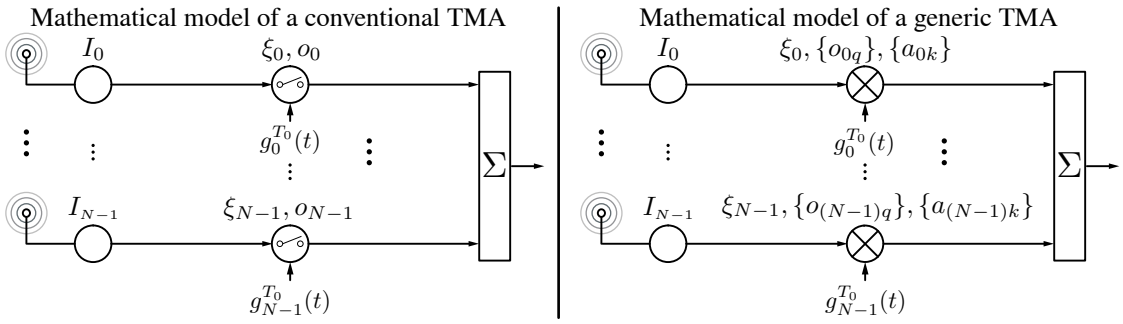

Fig. 1. Block diagrams of the mathematical model of a conventional TMA (left-hand side) and a generic TMA (right-hand side). A conventional TMA is a TMA implemented with on-off switches. The parameters that can be adjusted to optimize the array depend on its type. In a generic TMA, the involved parameters are ξ_n (normalize pulse durations), o_{nq} (normalize pulse time shifts), and a_{nk} (pulse weights), $n \in \{0, 1, \ldots, N-1\}$, $q \in \{0, \pm 1, \ldots, \pm L\}$, and $k \in \{0, 1, \ldots, K\}$, where L is the order of the highest exploited harmonic, and K is the order of the pulse.

frequency, which can be replicated and adapted in a chosen number of harmonic frequencies. That is the idea behind the so-called enhanced time-modulated array (ETMA), which is proposed in this paper and described in detail in Section II-B. Notice that the mathematical model of ETMAs fits into the generic TMA graphical description shown in Fig. 1 (right-hand side) in contrast to conventional TMAs shown in Fig. 1 (left-hand side).

The main contributions of this paper –taking as the departure point the introduction in [7]– are the following:

1) The quantification of the vulnerabilities of rectangular pulses in conventional TMAs for beamforming purposes.
2) The introduction of a novel signal processing procedure to obtain fully-independent TMA harmonic patterns, leading to unprecedented levels of flexibility and efficiency.
3) The description of a method for synthesizing ETMAs together with a demonstration showing that such a method is compatible with both classical nulling methods –based on exclusively perturbing the excitation phases– and pattern nulling algorithms –specifically designed for conventional TMAs.
4) The specification of the hardware required to implement ETMAs and a comparison to that employed by conventional TMAs.
5) A comparison in terms of power efficiency between the proposed ETMAs and existing conventional TMAs.

II. Impact of TMA Pulses on Harmonic Beamforming

Let us consider a linear TMA with N isotropic elements, each one modulated by a periodic (with fundamental period T_0) pulse $g_n^{T_0}(t)$ where $n \in \{0, 1, \ldots, N-1\}$. We assume that the beamforming is performed over the harmonic frequencies qf_0, with $q \neq 0$, $f_0 = 1/T_0$ being the TMA periodic pulse train fundamental frequency, and $q \in \{0, \pm 1, \pm 2, ..., \pm L\}$, where L is the order corresponding to the highest exploited harmonic. The array factor corresponding to the harmonic frequency qf_0 (with $q \neq 0$) is given by [8]

$$F_q(\theta, t) = \sum_{n=0}^{N-1} I_n G_{nq} \mathrm{e}^{jkz_n \cos\theta} \mathrm{e}^{j2\pi(f_c + qf_0)t}, \qquad (1)$$

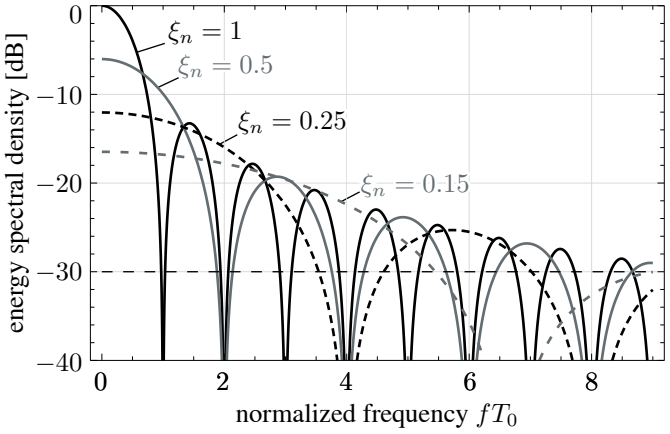

Fig. 2. Limitations on harmonics windowing with rectangular pulses. The figure shows the frequency-normalized ESD of a rectangular pulse, $|G_n(f)|^2$, for different values of ξ_n (normalized pulse widths). The squared amplitude of the n-th excitation corresponding to the q-th harmonic pattern, considering $|I_n| = 1$, can be graphically identified in the plot as $|I_{nq}^{\mathrm{TMA}}|^2 = G_{nq}^2 = |G_n(q)|^2$.

where z_n represents the n-th array element position on the z axis, $I_n = |I_n| \mathrm{e}^{j\varphi_n}$ is the complex representation of the per-antenna current static excitation, θ is the angle with respect to the main axis of the array, k is the wavenumber, and f_c is the carrier frequency.

A. Vulnerabilities of Rectangular Pulses

Given a rectangular pulse defined as

$$g_n(t) = \mathrm{rect}(t/\tau_n) = \begin{cases} 1 & t \in (-\tau_n/2, \tau_n/2) \\ 0 & \text{otherwise,} \end{cases} \qquad (2)$$

the periodic (T_0) extension of such a pulse admits the following exponential Fourier series representation

$$g_n^{T_0}(t) = \sum_{q=-\infty}^{\infty} G_{nq} \mathrm{e}^{jq\frac{2\pi}{T_0}t}, \qquad (3)$$

where G_{nq} are the exponential Fourier series coefficients. Since the Fourier transform of $g_n(t) = \mathrm{rect}(t/\tau_n)$ is $G_n(f) =$

$\tau_n \text{sinc}(\pi\tau_n f)$, the coefficients G_{nq} are given by

$$G_{nq} = \frac{1}{T_0} G_n(q/T_0) = \xi_n \,\text{sinc}(\pi q \xi_n), \tag{4}$$

with $\xi_n = \tau_n/T_0$ being the normalized pulse durations. In view of (1) and (4), it is found that

$$I_{nq}^{\text{TMA}} = I_n G_{nq} = I_n \xi_n \text{sinc}(\pi q \xi_n) \tag{5}$$

are the dynamic excitations of the q-th harmonic pattern of the TMA. Therefore, the design and optimization of TMAs for harmonic beamforming purposes using rectangular pulses unavoidably encounters the limitations imposed by the features of the sinc function, whose ESD exhibits the following properties (see Fig. 2 for $\xi_n = 1$): (a) a normalized main-lobe width (NMLW)[2] equal to 1, which is the minimum possible value; (b) a maximum side-lobe level (MSLL) of -13 dB; and (c) a first order $(1/f)$ spectrum roll-off or asymptotic decay.

In order to include successive harmonics (with normalized frequencies corresponding to $1, 2, 3 \ldots$) under the main lobe through time-modulation techniques, it is necessary to reduce the width of the pulses in the time domain by virtue of (a), but the desired windowing effect with the working harmonics –to avoid an efficiency penalty– is not achieved unless those pulse widths are close to zero due to (b) and (c). Under these circumstances, the power efficiency levels are safeguarded but, unfortunately, with pulse widths too close to zero, the TMA gain (and hence the SNR at the receiver) is reduced when compared to conventional linear beamforming solutions that synthesize the same pattern. Indeed, the average SNR of a signal received over the TMA q-th harmonic is proportional to the antenna gain in the direction of the radiation peak of such a pattern, G_q^{TMA} [9], i.e.,

$$\text{SNR}_q^{\text{TMA}} \propto \mathbf{G}_q^{\text{TMA}} = \eta_{\text{TMA}}^{\text{Rect}} \frac{4\pi |F_q(\theta_q, t)|^2}{P_{\text{R}}^{\text{TMA}}}, \tag{6}$$

where $\eta_{\text{TMA}}^{\text{Rect}}$ is the total efficiency of the TMA given by

$$\eta_{\text{TMA}}^{\text{Rect}} = \eta_s \eta(L), \tag{7}$$

with η_s the efficiency of the switching network accounting for the energy absorption when the switches are off, and $\eta(L)$ the TMA power efficiency when $L-1$ harmonics are exploited in addition to the fundamental mode. Such a power efficiency is defined as the ratio between the useful mean received power P_U^{TMA} and the total mean received power P_R^{TMA}, i.e.,

$$\eta(L) = \frac{P_{\text{U}}^{\text{TMA}}}{P_{\text{R}}^{\text{TMA}}} = \frac{\sum_{q=-L}^{L} p_q}{\sum_{q=-\infty}^{\infty} p_q}, \tag{8}$$

where $P_{\text{U}}^{\text{TMA}}$ and $P_{\text{R}}^{\text{TMA}}$ are the useful and total mean received power values, respectively, which can be expressed in terms of p_q, the total mean received power at the q-th harmonic when a carrier is received over the TMA [10]. In view of (8), the level of non-exploited harmonics must be kept below a certain level in order to efficiently achieve the appropriate values, which are close to 1. On the other hand, we can compare G_q^{TMA} to the gain of a static array (STA), G_q^{STA}, which accomplishes linear beamforming generating the same spatial radiation patterns $|F_q(\theta_q, t)|^2$ as the TMA, and thus having the same static excitations $I_{nq}^{\text{STA}} = I_{nq}^{\text{TMA}}$. We can express such a gain as

$$G_q^{\text{STA}} = \alpha_{\text{BFN}} \frac{4\pi |F_q(\theta_q, t)|^2}{P_{\text{R}}^{\text{STA}}}, \tag{9}$$

with α_{BFN} the attenuation of the STA beamforming network (BFN) and $P_{\text{R}}^{\text{STA}}$ the total mean received power for the STA. By considering an inter-element distance of $\lambda/2$, $|I_n|$=1, and according to [8, Eq. (42)]:

$$p_q = 4\pi \sum_{n=0}^{N-1} |G_{nq}|^2 = 4\pi \sum_{n=0}^{N-1} \xi_n^2 \text{sinc}^2(\pi q \xi_n), \tag{10}$$

and the following expression is easily obtained [10]

$$\frac{G_q^{\text{TMA}}}{G_q^{\text{STA}}} = \frac{\eta_{\text{TMA}}}{\alpha_{\text{BFN}}} \frac{\sum_{n=0}^{N-1} \xi_n^2 \text{sinc}^2(\pi q \xi_n)}{\sum_{n=0}^{N-1} \xi_n}. \tag{11}$$

This ratio shows –by simply analyzing any of the two ratios of the expression– that, with pulse durations ξ_n too close to zero, $G_q^{\text{TMA}} \ll G_q^{\text{STA}}$, hence yielding $\text{SNR}_q^{\text{TMA}} \ll \text{SNR}_q^{\text{STA}}$ after applying (6).

Regarding the excitation phases of the harmonic patterns, we easily arrive at a more generalized version of (4) when a non-even rectangular pulse $g_n(t)$ is considered and a normalized time-shift o_n is applied to $g_n^{T_0}(t)$ [2]

$$G_{nq} = \xi_n \,\text{sinc}(q\pi\xi_n) \text{e}^{-jq\pi(\xi_n + 2o_n)}. \tag{12}$$

Therefore, by substituting (12) into (5), we obtain the excitations for the successive harmonic patterns ($q \geq 1$) and we notice that the switching architecture imposes that harmonic patterns with different order exhibit a dependency between their phases. This property seriously limits the performance of a TMA in a realistic scenario where the direction of arrivals (DOAs) are random. In this sense, and more specifically, sophisticated multi-objective optimization methods [2, Section III-A] are used to shape the required beams under such a restriction, but the price to be paid is a serious degradation of the TMA power efficiency as it is shown in Section IV-B, which is devoted to calculate the TMA power efficiency in some of the designs existing in the recent literature.

In summary, the designer lacks of full freedom –due to the trade-off between flexibility and power efficiency– to assign the corresponding phases and synthesize a series of independent harmonic diagrams according to the adaptive beamforming.

B. SWC Pulses: The Enhanced TMA (ETMA) Concept

Due to the harmonic beamforming limitations of rectangular pulses described in the subsection above, our aim is to identify a pulse with the following properties:

1) easy generation in the time domain;
2) good windowing features, i.e., a frequency response with a main lobe containing a large part of the total energy, an MSLL as small as possible relative to the main-lobe peak, and side-lobes decaying asymptotically at an appropriate rate; and

[2]Note that the frequency axis is normalized with respect to the minimum pulse width $f_0 = 1/T_0$, which is the time-modulation frequency.

TABLE I
TMA MODES FOR HARMONIC BEAMFORMING DEPENDING ON THE CHARACTER OF THE VARIABLES OF THE SWC PULSES. PATTERN SYNTHESIS REQUIREMENTS ARE ALSO ILLUSTRATED.

TMA mode	type of parameter			optimization	
	ξ_n	o_{nq}	a_{nk}	type	complexity
conventional TMA	adaptive	adaptive	nonadaptive	systematic	high$^{(*)}$
enhanced TMA (ETMA)	nonadaptive	adaptive	adaptive	heuristic	low
advanced TMA	adaptive	adaptive	adaptive	systematic	high

(*): The terms "high" or "low" are qualitative more than quantitative. Therefore, in relative terms, the systematic optimization complexity is "high" compared to the heuristic optimization. The main reason is that the optimization level required in ETMAs is minimum as the initial pattern synthesized (two simple steps) already has an excellent efficiency.

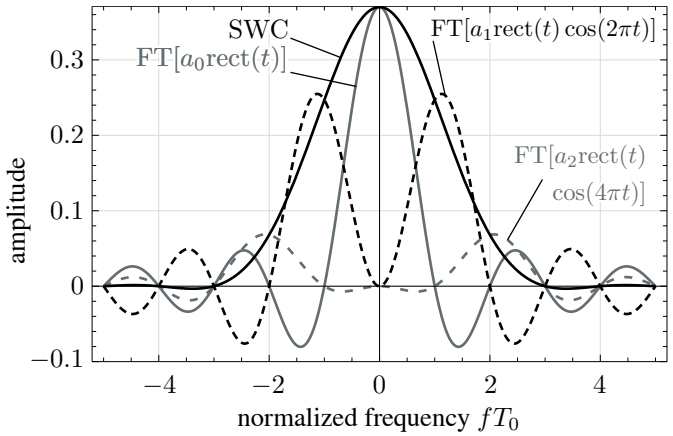

Fig. 3. Synthesis of a 3-term SWC pulse as a superposition of frequency-shifted rectangular pulses. The pulse is appropriate for efficiently exploiting the first and the second harmonics with a TMA. The weighting coefficients are $a_0 = 0.37$, $a_1 = 0.49$, and $a_2 = 0.14$.

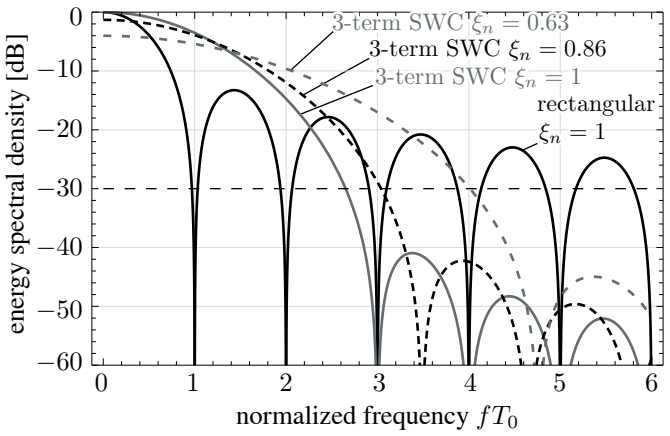

Fig. 4. Examples of ESD vs. normalized frequency curves for the 3-term SWC pulse of Fig. 3, $|G_n(f)|^2$, for different values of the normalized pulse durations ξ_n and comparison with the rectangular pulse (corresponding to the minimum width, $\xi_n = 1$). Analogously to Fig. 3, $|I_{nq}^{\text{TMA}}|^2 = |G_n(q)|^2$. As a result of the pulse windowing behavior, a selection of $0.86 \leq \xi_n \leq 1$ allows for working selectively with the fundamental mode, the first and the second harmonics, i.e., exploiting $|q| \leq 2$ while keeping below -30 dB the higher order harmonics. For $0.63 \leq \xi_n \leq 0.86$, the order of the harmonics selectively exploited are those with $|q| \leq 3$. Hence, in view of the pulse response, it is guaranteed a selective exploitation of the harmonics for certain intervals of ξ_n and fixed pulse weights a_{nk}. Additionally, for a given interval of ξ_n, it is possible to adjust both the harmonic selectivity (since the pulse bandwidth can be modified) and the levels of the selected harmonics by varying the pulse weights a_{nk}. An example of this adjustment is shown in Section IV.

3) flexibility to shape dynamically and independently the harmonic patterns.

Such a versatility would give us the possibility of obtaining high values for the TMA power efficiency while working with pulse widths close to 1, thus overcoming the aforementioned SNR deterioration. The superposition of frequency-shifted rectangular pulses, presented in the introduction and shown in Fig. 3 –the so called SWC pulses– seems to fit very well into the pulse idea we are seeking. Let us now proceed to present a generalized analysis about the use of SWC pulses in a TMA to exploit its harmonic patterns. In order to construct such periodic pulse trains, $g_n^{T_0}(t)$, we first define a basic pulse given by an SWC over a finite duration $\tau_n \leq T_0$

$$b_n(t) = \sum_{k=0}^{K} a_{nk} \cos(2\pi k t/\tau_n)\,\text{rect}(t/\tau_n), \tag{13}$$

where a_{nk} are real-valued constants with $k \in \{0, 1, \ldots, K\}$. K is the order of the basic pulse $b_n(t)$, and the constants a_{nk} satisfy the normalization condition

$$\sum_{k=0}^{K} a_{nk} = 1. \tag{14}$$

Recall that the pulses given by (13) have been used to design a widely known family of window functions with controllable side-lobe behavior [6].

Recall now that the exponential Fourier series representation of the periodic extension of the basic pulse in (13) is given by

$$b_n^{T_0}(t) = \sum_{q=-\infty}^{\infty} B_{nq} \mathrm{e}^{jq(2\pi/T_0)t}, \tag{15}$$

where

$$B_{nq} = \frac{1}{T_0} B_n\left(\frac{q}{T_0}\right) = \frac{\xi_n^2 q}{\pi} \sin(\pi \xi_n q) \sum_{k=0}^{K} \frac{(-1)^k a_{nk}}{\xi_n^2 q^2 - k^2} \tag{16}$$

are the Fourier series coefficients. This result is obtained from

$$B_n(f) = \frac{\tau_n^2 f}{\pi} \sin(\pi \tau_n f) \sum_{k=0}^{K} \frac{(-1)^k a_{nk}}{(\tau_n^2 f^2 - k^2)}, \tag{17}$$

which is the Fourier transform of $b_n(t)$ [6]. On the other hand, let us introduce an additional periodic (T_0) signal,

$v_n^{T_0}(t)$, which accounts for the phases of the excitations of the harmonic patterns given by

$$v_n^{T_0}(t) = 1 + \sum_{q=1}^{L} \cos\left(\frac{2\pi q}{T_0}\left(t - \delta_{nq}\right)\right), \tag{18}$$

where each δ_{nq} is a time-delay used as a design parameter to properly control the phase of the excitation of the n-th element of the q-th order harmonic pattern. Since $v_n^{T_0}(t)$ is a real-valued signal, its Fourier series coefficients satisfy the Hermitian symmetry property and are given by

$$V_{nq} = V_{n(-q)}^{*} = \mathrm{e}^{-j2\pi q(\delta_{nq}/T_0)} = \mathrm{e}^{-j2\pi q o_{nq}}, \tag{19}$$

with $o_{nq} = \delta_{nq}/T_0$ being the normalized time-delays. Finally, we construct $g_n^{T_0}(t)$ from the periodic convolution

$$g_n^{T_0}(t) = v_n^{T_0}(t) \circledast b_n^{T_0}(t), \tag{20}$$

whose Fourier series coefficients satisfy[3]

$$G_{nq} = V_{nq} B_{nq}. \tag{21}$$

By considering (16) and (21), we can identify in (1)

$$I_{nq}^{\mathrm{TMA}} = I_n \frac{\xi_n^2 q}{\pi} \sin(\pi \xi_n q) \sum_{k=0}^{K} \frac{(-1)^k a_{nk}}{\xi_n^2 q^2 - k^2} \mathrm{e}^{-jq2\pi o_{nq}} \tag{22}$$

as the dynamic excitations of the q-th harmonic pattern of the TMA.

Fig. 4 shows the ESD of the pulse synthesized in Fig. 3 for different values of ξ_n, as well as the comparison with the rectangular pulse (case of minimum width $\xi_n = 1$). Note that by considering $|I_n| = 1$, then $|I_{nq}^{\mathrm{TMA}}|^2 = |G_n(q)|^2 = |B_n(q)|^2$ (see (16), (21), and (22)). Fig. 4 shows the suitability of such an SWC pulse for an efficient exploitation of the first and the second order harmonics.

In view of (22), we have different degrees of freedom in the harmonic beamforming design depending on the static (nonadaptive) or dynamic (adaptive) nature of the variables involved. Therefore, and according to Table I, if a_{nk} are fixed while ξ_n and o_{nq} are adjusted dynamically, we have a so-called pure or conventional TMA. The radiation pattern optimization in this case is a sophisticated task based on multi-objective optimization methods (such as genetic algorithms, simulated annealing, or particle swarm) similar to those applied to the case of rectangular pulses. If additionally a_{nk} are dynamically adjusted –this is the case which we will henceforth refer to as advanced TMA– the problem has to be solved employing similar methods but with a larger number of parameters.

In order to have a more clear idea about the complexity of the systematic optimization methods to be applied for the synthesis of both conventional TMAs and advanced TMAs based on SWC pulses, we briefly describe a reference example with a specific method. Although such a method can be applied to conventional TMAs with rectangular pulses [2, Section III-A], it can be also adapted to TMAs based on SWC pulses by using the Fourier coefficients G_{nq} (see Eqs. (1) and (21)) for the SWC pulses. As already pointed out, such coefficients provide a new degree of freedom by means of a_{nk}. In the systematic method in [2, Section III-A] it is defined a fitness function [2, Eq. (10)] consisting of three weighted functionals accounting, respectively, for the following features of the radiation pattern: 1) the SLL of the beams, 2) the level of equalization between the maxima of the beams, and 3) the position of the nulls. Such a fitness function is optimized, in this case, through a particle swarm optimization (PSO) algorithm. We have classified the complexity of this technique (see Table I) as "high" in relative terms, i.e., when compared to the one described below and applied to a third type of TMAs with SWC pulses. Such a third alternative offers another possibility to perform adaptive beamforming by updating dynamically o_{nq} and a_{nk} while using the pulse time durations corresponding to the design of a quiescent (non-adaptive) pencil beam pattern in the fundamental frequency, which can be replicated and adapted in a chosen number of harmonic frequencies. That is the idea behind the ETMA, and its greatest advantage is the simplicity in the synthesis of the radiation diagrams, which is given by the the following procedure consisting of four steps:

1) Assign to ξ_n the values synthesizing a particular pattern for the fundamental mode (which, according to the particular SWC pulse response, will be properly replicated in the harmonic frequencies).
2) Compute the initial values for a_{nk} by means of the equations given in Section III-A, where K (the order of the pulses) depends on the number of harmonics L to be exploited.
   After these two steps, the achieved efficiency level is excellent (above 95 % in the examples in Section IV, summarized in the captions of Figs. 6 to 12). This is due to the adequate windowing features of SWC pulses in contrast to those exhibited by the rectangular pulses. The third and the fourth steps account for two extra features:
3) The possibility of using either classical nulling methods based on exclusively perturbing the excitation phases e.g. [11], or more recent and sophisticated ones [12], [13].
4) The optimization of the efficiency (becoming quasi-ideal) by strategically forcing to zero some a_{nk} of the array (see an example in Section IV, Fig. 7). In this regard, this is a heuristic mechanism that allows for looking for a sufficiently good –albeit not necessarily optimal– solution with a low computational complexity. Compared to systematic methods, we have described this last method as a "low" complexity one in Table I.

Once the three modes of exploitation have been described, and since the goal of this paper is to introduce the advantages of ETMAs based on SWC pulses, we will focus the forthcoming sections on ETMAs, leaving the case of advanced TMAs for future works.

[3]If $x(t)$ and $y(t)$ are periodic (T) signals, its periodic convolution $z(t)$ is defined as: $z(t) = x(t) \circledast y(t) = 1/T \int_{<T>} x(\tau) y(t-\tau) d\tau$ and if a_k, b_k are the Fourier series expansion coefficients of $x(t)$ and $y(t)$, respectively, then $c_k = a_k b_k$ are the corresponding coefficients of $z(t)$.

III. Harmonic Beamforming with ETMAs

A. TMA Synthesis Method

The idea behind an ETMA is the possibility of carrying out an efficient harmonic beamforming without needing the pulse durations ξ_n to be too close to zero, which would cause unavoidably a degradation in terms of power efficiency and, consequently, a loss in the SNR at the receiver. Additionally, ETMAs provide flexibility in the radiation pattern synthesis by governing the amplitude variable a_{nk}, together with the time variables ξ_n and o_{nq} according to (22).

The operational mode proposed for the ETMAs is based on the design of a quiescent pencil beam pattern in the carrier frequency by means of properly setting the $I_n\xi_n$ products according to [14]. The difference now is that, by means of the SWC pulses, it is possible to create replicas of such a pencil beam pattern at a given number of harmonic frequencies, with the novelty of using a_{nk} and o_{nq} to reconfigure these new diagrams adaptively according to (22). Under this assumption, ξ_n are time parameters involved in the design to improve the SLL in the quiescent pattern, but having a non adaptive character. On the other hand, note that since the phases of the excitations (caused by the time delays o_{nq}) of each harmonic pattern are independent, it is possible an autonomous application of pattern nulling methods to each harmonic diagram (see, for example, [11]). Another possibility is to use the existing methods for TMA nulling [12], [13], taking into account the new degrees of freedom introduced by the ETMA.

The radiation pattern synthesis procedure may exploit the following property of the Fourier Transform of an SWC pulse (16), (17) when $\xi_n = 1$

$$B_{nq}\Big|_{\xi_n=1} = \frac{1}{T_0} B_n\left(\frac{q}{T_0}\right)\Bigg|_{\xi_n=1} = \begin{cases} a_{n0} & q = 0 \\ a_{n|q|}/2 & q \neq 0; |q| \leq K \\ 0 & \text{otherwise,} \end{cases} \tag{23}$$

where K is the order of the basic SWC pulse in (13) and coincides with the highest order of the exploited harmonics, i.e., $K = L$. As mentioned before, the working interval for the TMA pulse durations ξ_n should be as close to 1 as possible for an efficient beamforming. On the other hand, it was analyzed in Section II-B, and also shown in Fig. 4, that the SWC pulses allow for windowing, with a good level of equalization, the corresponding working harmonics for certain intervals of ξ_n in the proximity of 1. Then, we can expect a behavior of B_{nq} –and therefore of $|I_{nq}^{\text{TMA}}| = |I_n||B_{nq}|$ (see (22))– according to (23) for a certain interval of ξ_n relatively close to 1, i.e., the excitation amplitudes of the q-th harmonic pattern of the TMA (with excitations $|I_{nq}^{\text{TMA}}|$) can be governed reliably by the set of coefficients $\{a_{0|q|}, a_{1|q|}, \ldots, a_{(N-1)|q|}\}$ corresponding to each of the N pulses. Under those circumstances, it is possible to design harmonic beams with similar amplitude patterns by properly choosing the coefficients a_{nk} in (23) as a starting point in the design. Hence, in order to obtain identical amplitude harmonic patterns, we should consider:

$$a_{n|q|} = 2a_{n0};\ |q| \leq K; q \neq 0 \text{ and } \forall n, \tag{24}$$

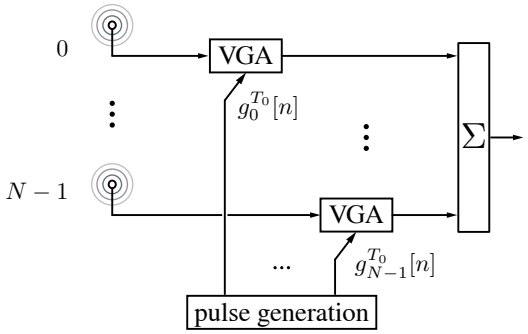

Fig. 5. Diagram of an ETMA for adaptive beamforming. Note that the hardware is the same as the one of a conventional TMA but replacing the RF switches with RF VGAs equipped with digital control.

and if we apply the normalization condition (14), we easily express (24) as

$$a_{n|q|} = 2a_{n0} = \frac{2}{2K+1}, \tag{25}$$

which is an initial condition to obtain equal excitation amplitudes $|I_{nq}^{\text{TMA}}|$, $\forall\ |q| \leq K$, and consequently, replicated harmonic patterns. Since the windowing level is not ideal, due to the presence of the $\xi_n \leq 1$ (see Fig. 4), the attenuation of the first unexploited harmonics must be improved. A great advantage of this technique is that it is easy to control the level of such unwanted harmonics by a certain adjustment of a_{nk} with respect to the values given by (25), as we illustrate in one of the examples presented in Section IV. Recall that the remaining unwanted harmonics are already properly attenuated due to the SWC pulses spectral shape (see Fig. 4).

B. TMA Hardware Structures

In this section we analyze possible hardware structures for the ETMA based on SWC pulses. Additionally, they are compared to the corresponding architecture of conventional TMAs based on RF switches. The available solutions are:

1) **RF variable gain amplifiers (VGAs) with digital control**. An initial potential implementation for the ETMA is the one proposed in [15] and illustrated in Fig. 5. Such a structure was originally proposed to implement a beamforming method using pure sinusoids [15] and presented as an alternative to beamforming with TMA. Notice that it has the same structure as a conventional TMA but replacing the RF switches with RF VGAs with digital control. Recall that, as the pulses must be generated in the digital domain in any implementation of a TMA, we consider the same control unit or digital signal processor (DSP) for all the implementations presented here (including the TMA with RF switches). This very simple architecture is a reasonable choice for beamforming because it provides much better features –albeit increased power consumption– than the implementation based on RF switches.
2) **RF VGAs with analog control and digital-to-analog converters (DACs)**. According to the scheme shown in Fig. 5, it is possible to use VGAs with analog control,

but additional DACs are required. This solution is more expensive than the previous one, being the cost inversely related to the power consumption of the VGAs. The DACs imply an extra cost but at least exhibiting a low power consumption. The architecture is more complex than the one in Fig. 5 although still quite simple.

3) **RF multipliers with DACs**. The multipliers have a power consumption slightly higher than that of the VGAs with digital control for the same frequency, but with twice the cost. However, they are a competitive solution with respect to the VGA with analog control.

On the other hand, let us consider an adequate structure for the TMA based on RF switches envisaged for beamforming purposes:

4) **Conventional TMAs**. The appropriate type of switches to be considered, in order to carry out a fair comparison in terms of hardware, are the so-called single-pole triple-throw (SP3T) switches. A common denominator in this article is that the harmonic beamforming must be capable of safeguard the TMA power efficiency. In this sense, the use of a single RF switch for the control of two adjacent elements allows for improving the switching network efficiency whenever pairs of complementary pulses are synthesized [9]. Therefore, in order to exploit up to three beams, it is only possible to achieve an adequate power efficiency level in the switching network (related to the fraction of the time that the switches are off), by using SP3T switches. For each switch, two throws are connected to a consecutive pair of array elements. For the case $L = 2$, the third throw will not be programmed or used, whereas for the case $L = 3$, such a throw is used as the off state.

Table II shows a comparison of the systems described above for TMA beamforming. Such a comparison is based, apart from the complexity of the hardware architecture, on key hardware parameters like power consumption, cost, and size.

Notice that, from a signal processing point of view, the TMA technique carries out a nonlinear transformation (contrarily to a linear beamforming network (LBFN)) in the analog domain independently from the devices employed: switches, VGAs, multipliers, etc. Such a nonlinear transformation in the analog domain is determined by the application of periodic pulses at the antenna level and its effects (conversion of space diversity into frequency diversity) can be profitably exploited by using a single RF front end. With this in mind, we can briefly compare the ETMA (as a representative example of the TMA technique, because the comparison is valid for any of the aforementioned implementations) with conventional analog and digital beamforming schemes. Accordingly, we first consider a conventional array with N elements provided with an analog LBFN prepared to exploit up to L beams. Such an LBFN will have $L \times N$ phase shifters and $L \times N$ VGAs. Additionally, the receiver must be provided with L independent RF chains and L analog-to-digital converters (ADCs). In this sense, any TMA solution consisting of a single RF chain and a single ADC avoids practical problems related to synchronization and phase coherence. The same reasoning applies to the problem of coupling between RF chains. On the other hand, in a fully digital implementation of an LBFN, the number of required RF chains, L, is equal to the number of antenna elements N. When N is large, however, having an RF chain per antenna is unfeasible due to a number of reasons, being the power consumption per element in the RF front-end one of the most important ones as shown in [16, Table I]. In fact, beamforming with hybrid analog-digital architectures is currently becoming an increased trend.

In order to clarify the feasibility of ETMA synthesis with VGAs based on SWC pulses instead of pure sinusoids as in [15], let us analyze more in detail –also in the frequency domain– the parallelism between both beamforming techniques based on VGAs: ETMAs and periodical amplitude modulation [15].

The sinusoidal function $U_n(t) = A_n\,(1 + \cos(f_0 t + \varphi_n))$ in [15, Eq. (2)] governing the n-th VGA becomes, in the ETMA version, the function $g_n^{T_0}(t)$ (see (20)), also periodic but with its spectrum being a train of Dirac deltas not only consisting of "lines" at frequencies $-f_0$, 0, and f_0 as U_n of [15], but also at frequencies $-2f_0$, $2f_0$, $-3f_0$, $3f_0$, …, for which the level of windowing of the SWC was designed by means of the a_{nk} values. The amplitude A_n in [15, Eq. (2)] determines the level of the spectral lines in $-f_0$, 0, and f_0, whereas for the ETMAs such a level is given by the Fourier coefficients G_{nq} (see (21)), which depend on ξ_n, a_{nk}, and o_{nq}, hence providing a powerful flexibility to the beamforming method.

Therefore, the applicability of the technique does not depend on the pure sinusoid character of the signals governing the VGAs. However, for both, pure sinusoids $U_n(t)$ and more complex periodic signals as $g_n^{T_0}(t)$, VGAs must satisfy the following conditions in the time domain:

- Their response time must be fast enough to follow $U_n(t)$ or $g_n^{T_0}(t)$. Therefore, the data acquisition frequency of the VGAs digital control signal must be high enough when compared to f_0. More specifically, greater than or equal to $N_s f_0$, being N_s the number of samples per period of $U_n(t)$ or $g_n^{T_0}(t)$. For the case of VGAs with analog control the response time is specified in terms of a full scale step or a 3 dB gain step, which is the delay or time response corresponding to such abrupt variations. SWC pulses are windowing functions characterized, precisely, by smooth variations (and also its periodic convolution with a cosine), avoiding the introduction of important issues in this technique. In any case, the time response must be chosen relatively low enough when compared to T_0 to guarantee a correct behavior.
- They must faithfully replicate the amplitude levels of the control input signal ($U_n(t)$ or $g_n^{T_0}$). For the case of VGAs with digital control the so-called gain step must be low enough to avoid quantification and distortion errors, whereas for the case of analog VGA control the linear gain specifications must be adequate.

IV. Results

We now present results that illustrate how the ETMA allows for achieving a twofold objective: (a) to exploit dynamically

TABLE II
HARDWARE COMPARISON OF THE BEAMFORMING NETWORKS IMPLEMENTED WITH TMAS.

		simple structure	cost	power consumption	size
conventional TMA	**RF switches**	excellent	excellent	excellent	excellent
enhanced TMA (ETMA)	**RF VGAs with digital control**	excellent	excellent	good	excellent
	RF VGAs with analog control	good	fair	good(*)	good
	multipliers	good	good	good	good

(*): Power and cost are inversely related.

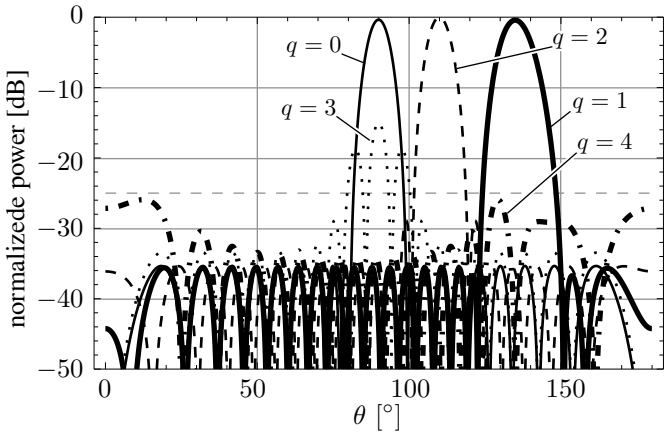

Fig. 6. Radiation Pattern of an ETMA without adjusting a_{nk}. Array with $N = 20$ achieving beamforming ($\theta_0 = 90°$, $\theta_1 = 135°$, and $\theta_2 = 110°$) over the first and the second harmonics. The TMA uses 3-term SWC pulses ($K = 2$) with weights (see (25)): $a_{n1} = a_{n2} = 2a_{n0} = 2/5$. Hence $\mathrm{SLL}_0 = -35\,\mathrm{dB}$, $\mathrm{SLL}_1 = -35\,\mathrm{dB}$, and $\mathrm{SLL}_2 = -28\,\mathrm{dB}$. The maximum unwanted harmonic peak is $-15\,\mathrm{dB}$, with $P_0 = 19.24\,\%$, $P_{|1|} = 38.09\,\%$, and $P_{|2|} = 40.82\,\%$, yielding $\eta(L) = 98.15\,\%$, $E[\xi_n] = 0.88$, and $S[\xi_n] = 0.12$.

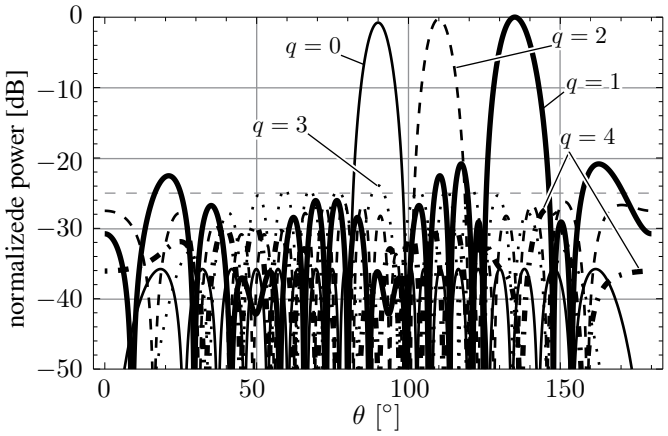

Fig. 7. Adjusted radiation pattern of an ETMA ($N = 20$) achieving beamforming ($\theta_0 = 90°$, $\theta_1 = 135°$, and $\theta_2 = 110°$) over the first and the second order harmonics. The TMA uses 3-term SWC pulses ($K = 2$) with weights (see (25)): $a_{n1} = a_{n2} = 2a_{n0} = 2/5$ for $n \in [3, 16]$ and $a_{n0} = 1/5$, $a_{n1} = 4/5$, and $a_{n2} = 0$ for the rest of the elements. Hence $\mathrm{SLL}_0 = -35\,\mathrm{dB}$, $\mathrm{SLL}_1 = -22\,\mathrm{dB}$ and $\mathrm{SLL}_2 = -27\,\mathrm{dB}$. The maximum harmonic peak is $-25\,\mathrm{dB}$, with $P_0 = 22.34\,\%$, $P_{|1|} = 41.42\,\%$, and $P_{|2|} = 35.15\,\%$, yielding $\eta(L) = 98.91\,\%$, $E[\xi_n] = 0.88$, and $S[\xi_n] = 0.12$.

the first and the second order harmonic patterns with an adequate SLL, and (b) to achieve higher power efficiency levels, and thus higher average SNR at the receiver, than those obtained with rectangular pulses.

A. Beamforming Design for Time-Varying Scenarios

Let us consider a linear array with $N = 20$ antennas and an inter-element separation $d = \lambda/2$. The antenna excitations I_n are chosen to synthesize a Dolph-Chebyshev (DC) pattern with an $\mathrm{SLL} = -30$ dB. The beamforming design is organized in three steps:

- **Selection of** ξ_n. Since $I_{n0}^{\mathrm{TMA}} = I_n \xi_n$ (see (22)), the elements of the array are time-modulated by the periodical pulses in (20) to improve the SLL of the fundamental mode [14]. We seek for an additional improvement of the SLL that, thanks to the SWC pulses, will be translated to all the harmonic patterns. In this example, a set of $\xi_n \in [0.59, 1]$, with a mean value $E[\xi_n] = 0.88$ and a standard deviation $S[\xi_n] = 0.12$, allows for an initial 5 dB SLL improvement of the working patterns, i.e., I_{n0}^{TMA} corresponds to the excitations of a DC pattern with $\mathrm{SLL} = -35\,\mathrm{dB}$.
- **Initial** a_{nk}. In this example the first and the second order harmonics are exploited, and hence $K = 2$ is considered together with 3-term SWC pulses. As a first approach, and according to (25), we take the following weights for such pulses and for all n: $a_{n1} = a_{n2} = 2a_{n0} = 2/5$. Fig. 6 illustrates the beamforming results for the fundamental mode and the first four harmonics[4]. Recall that we have the possibility of pointing the maximum of each harmonic diagram independently through o_{nq}. In this case, we consider a scenario where $\theta_1 = 135°$ and $\theta_2 = 110°$.
  It is apparent from Fig. 6 the excellent SLL behavior exhibited by all patterns. Nevertheless, although the power efficiency is high ($\eta(L) = 98.15\,\%$), the peak level of the third harmonic ($-15\,\mathrm{dB}$) is too high and has to be improved.
- **Adjustment of** a_{nk}. As stated in Section III, and by virtue of (23), the amplitude of each excitation of the radiation pattern of the q-th harmonic ($|I_{nq}^{\mathrm{TMA}}|$) is proportional to the corresponding SWC pulse coefficient a_{nq}. In particular, $|I_{nK}^{\mathrm{TMA}}|$, which governs the highest

[4]As $g_n^{T_0}(t)$ is a real-valued signal, its Fourier coefficients verify $G_{nq} = G_{n(-q)}^*$, and it is easy to prove (see (1)) that $|F_q^{\mathrm{TMA}}(\theta, t)|^2 = |F_{-q}^{\mathrm{TMA}}(180° - \theta, t)|^2$, synthesizing a couple of diagrams for q and $-q$, which are symmetric with respect to $\theta_0 = 90°$. For the sake of simplicity, we do not represent the "$-q$" harmonic versions.

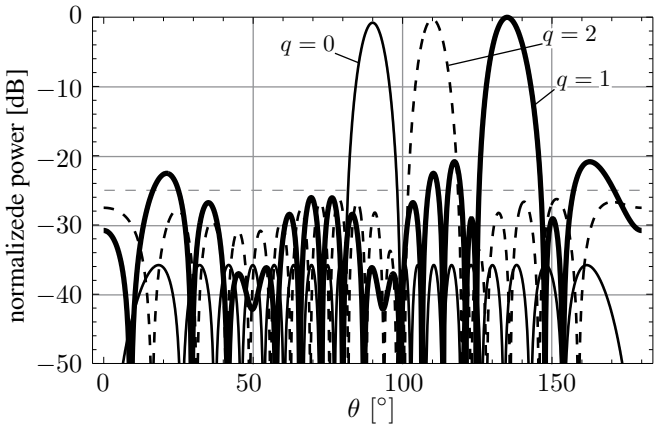

Fig. 8. Radiation pattern shown in Fig. 7 but without plotting the harmonics with order $q = 3$ and $q = 4$ for a major clarity of the previous situation before applying the adaptive nulling.

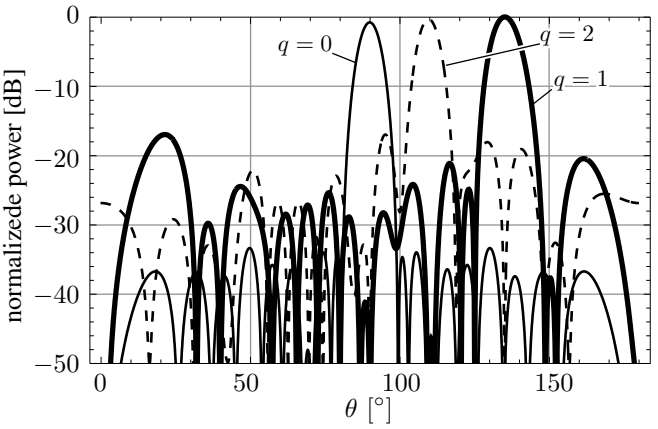

Fig. 9. Radiation pattern shown in Fig. 8 after the application of the adaptive nulling algorithm in [12], [13].

order harmonic pattern, is proportional to a_{nK}. Hence, by forcing a_{nK} to zero in the n-th SWC pulse (thus reducing its order to $K-1$), its shape will ensure a null contribution of the K-th harmonic and, additionally, a properly attenuated level of the $(K+1)$-th harmonic –due to the features of the SWC windowing function– once applied to the corresponding n-th element of the array. It is observed that by forcing a_{nK} to zero only in those pulses applied to the most distant elements of the center of the linear array, it is possible to reduce the peak level of the third harmonic to $-25\,\mathrm{dB}$ (see Fig. 7). In this case, such a simple adjustment leads to $a_{n0} = 1/5$, $a_{n1} = 4/5$, and $a_{n2} = 0$ for the last three elements placed at both ends of the linear array. It is also observed that the adjustment slightly modifies the total power distribution among the different harmonics, transferring approximately $5\,\%$ of the power from the third ($|q| = 2$) to the other patterns ($|q| = 1$ and $q = 0$). The consequent improvement in the efficiency ($\eta(L) = 98.91\,\%$) is at the expense of a certain SLL degradation of the harmonic patterns: $\mathrm{SLL}_1 = -22\,\mathrm{dB}$, $\mathrm{SLL}_2 = -27\,\mathrm{dB}$, whereas such a parameter remains intact for the fundamental mode: $\mathrm{SLL}_0 = -35\,\mathrm{dB}$.

Once the patterns are synthesized, it is possible to dynamically exploit them in time-varying scenarios where adaptive beamforming is needed. The adaptive beamforming can be performed basically in terms of adaptive nulling because the harmonics are capable of pointing their maximums independently. The pattern nulling can be performed according to the method proposed in [12], [13] but properly adapted to the ETMA. The method jointly optimizes the TMA parameters to synthesize a given pattern with predefined nulls.

In Fig. 8 we show the same pattern as the one in Fig. 7 but without plotting the harmonics with order $q = 3$ and $q = 4$ for the sake of clarity. Fig. 9 illustrates that it is possible to obtain mutual orthogonalization in a given radiation pattern by placing nulls at the angles corresponding to the maxima of the other diagrams, e.g. to exploit the TMA in a multipath communication. Notice that, for a given pattern, the directions of the corresponding maxima of the other ones are treated (in terms of nulling) as interference directions for this particular application, although we could have chosen any other spatial position for the nulls.

Because harmonic patterns with different order are independent between their phases (see (22)), in practice it is possible to introduce the nulls as in [12], [13] by changing only the phases of the excitations (in this case the average fluctuation of coefficients a_{nk} are below $1.77\,\%$). Therefore, when $d = \lambda/2$, as the excitation phases are not present in p_q (10) and, consequently, also not in (8), the nulling method does not impact on the power efficiency.

B. Power Efficiency of SWC and Rectangular Pulses

We have shown the high levels of power efficiency achieved by ETMAs based on SWC pulses. However, to complete the study, a comparison –in terms of power efficiency– between ETMAs based on SWC pulses and conventional TMAs based on rectangular pulses is included, provided that the same harmonic beamforming patterns are synthesized with both approaches.

The TMA power efficiency, when SWC pulses are used, is given by $\eta_{\mathrm{TMA}}^{\mathrm{SWC}} = \eta_{\mathrm{HW}} \cdot \eta(L)$, being η_{HW} the losses or the internal power dissipation in the hardware devices given in Table II, and $\eta(L)$ the power efficiency, described in Section II-A and calculated by means of (8). For $d = \lambda/2$, we compute the total mean received power at the q-th harmonic when a carrier is received over the TMA, denoted as p_q, in (8) as it is done in [8, Eq. 42],

$$p_q = 4\pi \sum_{0}^{N-1} |I_n|^2 |G_{nq}|^2 = 4\pi \sum_{0}^{N-1} \left|I_{nq}^{\mathrm{TMA}}\right|^2, \qquad (26)$$

with I_{nq}^{TMA} given in (22). We focus the study on the maximum efficiency of the TMA dictated by $\eta(L)$. The reason is that η_{HW} takes an arbitrary value depending on the specific properties of the hardware employed. Analogously, the analysis of the efficiency of a conventional TMA with switches is also addressed in terms of the power efficiency $\eta(L)$ also due to the arbitrary switching network efficiency, which depends on

the specific structure chosen, and may be based on single-pole single-throw (SPST) or single-pole multiple-throw (SPMT) switches or even on a Reconfigurable Power Divider/Combiner (RPDC) [17].

From now on we consider three examples of harmonic beamforming pattern synthesis that can be found in the recent literature. Particularly, such patterns have been synthesized through TMAs with rectangular pulses [2, Figs. 6, 10, and 11]. Our aim is twofold. Firstly, we synthesize the patterns through ETMAs based on SWC pulses, satisfying the same requirements in terms of DOAs, relative levels of maxima, and SLL. Secondly, the power efficiency exhibited by ETMAs based on SWC pulses is compared to that offered by the TMAs with rectangular pulses.

- **Example 1: ETMA versus optimized[5] TMA with two beams.** The TMA synthesized in [2, Fig. 6] performs harmonic beamforming by exploiting the fundamental and the first order harmonics ($L = 1$), whereas its pulse sequences are the result of a PSO optimization procedure –in terms of the radiation diagram shape– which is specifically defined in [2, Section II-2]. The multiobjective fitness function for such a PSO contemplates the SLL of the diagrams, the "equalization among the pattern maxima," and the mutual orthogonalization between patterns. In other words, the location of nulls of one pattern right in the direction of the maxima of the others[6].

  In the scenario considered, the maxima of the fundamental and first harmonic patterns, pointing to the corresponding DOAs, are respectively pointed towards the directions $\theta_0 = 90^\circ$ and $\theta_1 = 61^\circ$. In this example, a handicap for the time-modulation technique is the presence of uniform static excitations (which lacks of amplifiers and phase shifters) with $|I_n| = 1$ and zero-phase. Hence, the transformation of a simple static uniform pattern (with a modest $-13\,$dB SLL pattern) into the one shown in [2, Fig. 6(b)] is done, exclusively, by applying the time-modulation with rectangular pulses (whose features –see [2, Fig. 6(a)]– are the result of the PSO). The mean and the variance of the set of ξ_n necessary for this synthesis are equal to $E[\xi_n] = 0.1344$ (relatively close to 0) and $S[\xi_n] = 0.0074$, respectively. By substituting ξ_n into (10), we can compute p_q as well as the power efficiency by means of (8), arriving at $\eta(L) = 51.36\,\%$.

  Now, and for comparison purposes, we synthesize a pattern with the same characteristics as in [2, Fig. 6] by employing an ETMA. Firstly, we must obtain, through the application of time modulation, a pencil beam pattern in the fundamental frequency –which will be replicated in the first harmonic frequency– with an SLL about $-22\,$dB. We have chosen a DC pattern with an SLL of $-23\,$dB (other alternatives for pencil beam patterns are also valid, e.g., a normalized Gaussian pattern with a standard deviation of $2/3$). The set of ξ_n that synthesizes such a DC pattern has the following statistic properties: $E[\xi_n] = 0.7540$ (relatively closed to 1) and $S[\xi_n] = 0.0380$. According to the procedure described in Section IV-A to exploit $L = 1$ harmonic beams, we use $N = 20$ identical SWC pulses with order $K = L = 1$ and, as indicated in (25), $a_{n1} = 2a_{n0} = 1/3$.

  Fig. 10 illustrates the radiation pattern of this ETMA with the same characteristics as the one in [2, Fig. 6]. The power efficiency, calculated by means of (26) and (8), is now $\eta(L) = 95.41\,\%$, which significantly improves the efficiency achieved with rectangular pulses ($\eta(L) = 51.36\,\%$). Notice that there is still room for a heuristic optimization of the power efficiency adjusting the appropriate trade-off between the SLL of the DC pattern (modifying ξ_n) and certain slight variations of a_{nk}, as shown in Section IV-A.

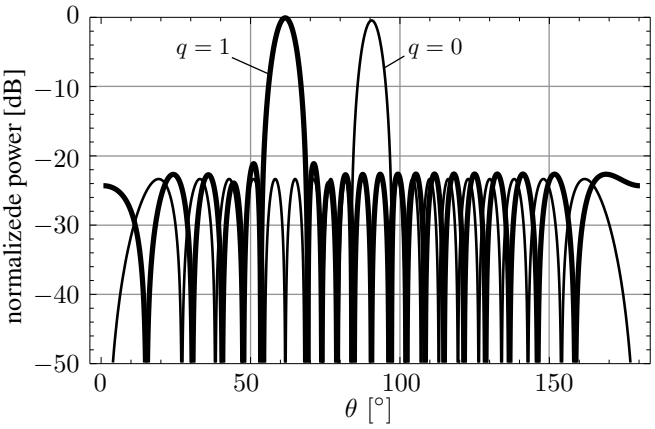

Fig. 10. Radiation pattern of an ETMA synthesized by applying identical 2-term SWC pulses with $a_{n0} = 2/3$, $a_{n1} = 2$ and normalized time durations ξ_n capable of synthesizing a DC pencil beam pattern with $\mathrm{SLL} = -23\,$dB. Such a pattern is equivalent to the one in [2, Fig. 6], synthesized with rectangular pulses and optimized by means of PSO. The power efficiency of the TMA is $\eta(L) = 51.36\,\%$, whereas that of the ETMA (even without optimization) improves noticeably up to $\eta(L) = 95.41\,\%$, yielding a relative improvement of $85.77\,\%$.

- **Example 2: ETMA versus non-optimized TMA with three beams.** The TMA synthesized in [2, Fig. 10] exploits the fundamental, the first, and the second order harmonics ($L = 2$) in a scenario where the maxima of the fundamental, the first, and the second harmonic patterns point to the corresponding DOAs, which are respectively pointed towards the directions $\theta_0 = 90^\circ$, $\theta_1 = 116^\circ$, and $\theta_2 = 150^\circ$.

  The corresponding pulse sequences have a fixed duration $\xi_n = 0.25$ and the switch-on time-instants are sequentially chosen as shown in [2, Fig. 10(b)]. The power efficiency, calculated analogously to the previous example for rectangular pulses, is $\eta(L) = 85.79\,\%$.

[5]In this case the optimization is referred to the shape of the radiation diagram, without taking the power efficiency of the array into account.

[6]Notice that the efficiency of an ETMA, with $d = \lambda/2$, does not change when applied to the adaptive nulling algorithm presented in [12], [13]. As explained at the end of Section IV-A, such an algorithm particularized for ETMAs is focused on the optimization of the independent (advantage of ETMAs with respect to conventional TMAs) excitation phases of the harmonic patterns. Due to the fact that such phases are not included in the efficiency (see (8) whenever $d = \lambda/2$ (case of the three examples below), the nulling method has no impact on the efficiency. As the aim of this section consists in showing the efficiency of ETMAs, it is not necessary to locate the nulls at the end of the synthesis, like it was properly done in the example in Section IV-A.

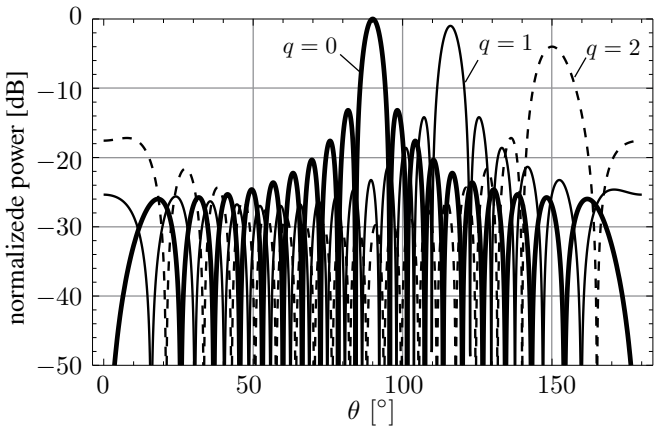

Fig. 11. Radiation pattern of an ETMA synthesized by applying identical 3-term SWC pulses with $a_{n0} = 0.2473$, $a_{n1} = 0.4407$, $a_{n2} = 0.3120$, and normalized time durations $\xi_n = 1$, hence the ETMA works under a degenerated mode where only the time shifts take part in the technique. The pattern of the figure is equivalent to the one in [2, Fig. 10], synthesized with rectangular pulses and showing an efficiency $\eta(L) = 85.79\,\%$. The ETMA, operating under this degenerated mode, exhibits its theoretical maximum efficiency, i.e., $\eta(L) = 100.00\,\%$, yielding a relative improvement of $16.56\,\%$.

It is observed in [2, Fig. 10] that the fundamental pattern corresponds to a uniform distribution (with an $\mathrm{SLL} = -13\,\mathrm{dB}$), and the harmonic patterns are attenuated replicas of such a pattern. Hence, it is possible to synthesize this pattern through an SWC-based infrastructure by simply choosing $\xi_n = 1$ and varying exclusively o_{nq}. In this sense, it is remarkable that when the beams correspond to uniform patterns, the synthesis can be carried out by using a degenerated mode of the ETMA, i.e., a mode of operation in which the time modulation is performed exclusively through the time shifts defined in (19) and fixing $\xi_n = 1$. Under this circumstances, the relationship given in (23) is perfectly satisfied, with B_{nq}^2 the level of the maximum of the q-th harmonic radiation pattern, whenever the N pulses are identical.

We use $N = 20$ identical SWC pulses with order $K = L = 2$, and therefore, the coefficients a_{nk} can be calculated by considering the attenuations –expressed in decibels– of the maximum of each harmonic pattern with respect to the maximum of the fundamental pattern [2, Fig. 10] ($-1\,\mathrm{dB}$ and $-4\,\mathrm{dB}$, respectively) by using the immediate equations: $20\log(B_{n1}/B_{n0}) = 20\log(a_{n1}/2a_{n0}) = -1$, $20\log(B_{n2}/B_{n0}) = 20\log(a_{n2}/2a_{n0}) = -4$, and the normalization condition in (14). Once solved this simple system of equations we obtain $a_{n0} = 0.2473$, $a_{n1} = 0.4407$, and $a_{n2} = 0.3120$. The theoretical power efficiency in an ETMA operating under the degenerated mode is $\eta(L) = 100.00\,\%$ because (23) is fully satisfied and the harmonic levels are zero for $|q| > K$. This fact can be proved by calculating the efficiency by means of (26) and (8).

Fig. 11 illustrates the radiation pattern of this ETMA with the same characteristics as that in [2, Fig. 10].

- **Example 3: ETMA versus optimized TMA with three beams.** The TMA synthesized in [2, Fig. 11] performs harmonic beamforming by exploiting the fundamental, the first, and the second order harmonics ($L = 2$), being the rectangular pulse sequences the result of the same PSO optimization procedure as in the first example. The DOAs scenario is the same as the one in the second example: $\theta_0 = 90°$, $\theta_1 = 116°$, and $\theta_2 = 150°$. The features of the pulse sequences applied to the static uniform excitations in order to obtain the diagram in [2, Fig. 11(a)] are shown in [2, Fig. 11(c)] and they are the result of the PSO. The mean and the variance of the set of ξ_n necessary for this synthesis are $E[\xi_n] = 0.0996$ (very closed to 0) and $S[\xi_n] = 0.0013$, respectively. Following the same procedure as in previous examples to calculate the power efficiency we arrive at $\eta(L) = 50.41\,\%$.

  An ETMA with the same pattern characteristics as in [2, Fig. 11(a)] can be synthesized by means of time-modulation with SWC pulses. The first step in the design consists in obtaining a pencil beam pattern in the fundamental frequency –which will be replicated or quasi-replicated in the first and in the second harmonic frequencies– with an SLL closed to $-22\,\mathrm{dB}$ as in the first example. We have also chosen a DC pattern with $\mathrm{SLL} = -23\,\mathrm{dB}$. Therefore, the set of ξ_n that synthesizes such a DC pattern are the same as those considered in the first example. To exploit $L = 2$ harmonic beams we employ $N = 20$ identical SWC pulses with order $K = L = 2$ and, as indicated in (25), $a_{n2} = a_{n1} = 2a_{n0} = 1/5$. Fig. 12 illustrates the radiation pattern of this ETMA with the same characteristics as the one in [2, Fig. 11] regardless of the location of the nulls, which, as it was properly explained, does not impact on the power efficiency in this example. The power efficiency, calculated as in previous examples, is now $\eta(L) = 97.16\,\%$ which, again, significantly improves the efficiency achieved by means of rectangular pulses ($\eta(L) = 50.41\,\%$).

V. Conclusions

We have proposed a novel family of TMAs, termed enhanced TMAs (ETMAs), whose excitations are time modulated by SWC pulses rather than by rectangular pulses corresponding to the on-off switches of conventional TMAs. We have presented the relationship between the harmonic radiation patterns and the SWC pulse parameters, as well as the TMA synthesis method. We have discussed some possible hardware structures for the implementation of ETMAs which have been properly compared to both conventional TMAs and LBFNs. We have shown that time modulation with periodic SWC pulses provides a larger flexibility to control the harmonic radiation patterns and, consequently, improves both the TMA power efficiency and the SNR at the receiver when compared to conventional TMAs based on rectangular pulses.

References

[1] H. E. Shanks and R. W. Bickmore, "Four-dimensional electromagnetic radiators," *Canadian Journal of Physics*, vol. 37, no. 3, pp. 263–275, 1959.

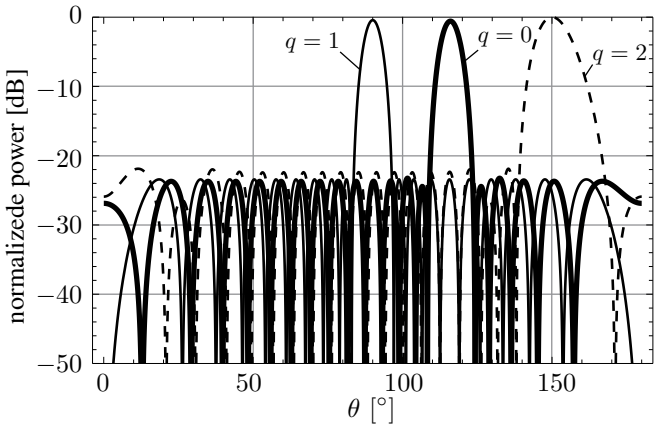

Fig. 12. Radiation pattern of an ETMA synthesized by applying identical 3-term SWC pulses with $a_{n2} = a_{n1} = 2a_{n0} = 1/5$ and normalized time durations ξ_n capable of synthesizing a DC pencil beam pattern with $\mathrm{SLL} = -23\,\mathrm{dB}$. Such a pattern is equivalent to the one in [2, Fig. 11], synthesized with rectangular pulses and optimized by means of the PSO. The power efficiency of the TMA is $\eta(L) = 50.41\,\%$, whereas that of the ETMA (even without optimization) improves noticeably up to $\eta(L) = 97.16\,\%$, yielding a relative improvement of $92.74\,\%$.

[2] P. Rocca, Q. Zhu, E. Bekele, S. Yang, and A. Massa, "4-D arrays as enabling technology for cognitive radio systems," *IEEE Transactions on Antennas and Propagation*, vol. 62, no. 3, pp. 1102–1116, March 2014.

[3] R. Maneiro-Catoira, J. Bregains, J. Garcia-Naya, and L. Castedo, "Time-modulated arrays for digital communications in multipath scenarios," in *2015 IEEE International Symposium on Antennas and Propagation USNC/URSI National Radio Science Meeting*, July 2015, pp. 816–817.

[4] L. Poli, P. Rocca, G. Oliveri, and A. Massa, "Harmonic beamforming in time-modulated linear arrays," *IEEE Transactions on Antennas and Propagation*, vol. 59, no. 7, pp. 2538–2545, July 2011.

[5] Y. Tong and A. Tennant, "A two-channel time modulated linear array with adaptive beamforming," *IEEE Transactions on Antennas and Propagation*, vol. 60, no. 1, pp. 141–147, Jan 2012.

[6] A. H. Nuttall, "Some windows with very good sidelobe behavior," *IEEE Transactions on Acoustics, Speech and Signal Processing*, vol. 29, no. 1, pp. 84–91, Feb 1981.

[7] R. Maneiro-Catoira, J. Bregains, J. Garcia-Naya, and L. Castedo, "Time-modulated arrays with sum of weighted cosine pulses," in *2016 IEEE International Symposium on Antennas and Propagation USNC/URSI National Radio Science Meeting*, July 2016, p. accepted for publication.

[8] R. Maneiro-Catoira, J. Brégains, J. García-Naya, and L. Castedo, "On the feasibility of time-modulated arrays for digital linear modulations: A theoretical analysis," *IEEE Transactions on Antennas and Propagation*, vol. 62, no. 12, pp. 6114–6122, Dec. 2014.

[9] Q. Zhu, S. Yang, R. Yao, and Z. Nie, "Gain improvement in time-modulated linear arrays using SPDT switches," *IEEE Antennas and Wireless Propagation Letters*, vol. 11, pp. 994–997, 2012.

[10] J. Bregains, J. Fondevila-Gomez, G. Franceschetti, and F. Ares, "Signal radiation and power losses of time-modulated arrays," *IEEE Transactions on Antennas and Propagation*, vol. 56, no. 6, pp. 1799–1804, 2008.

[11] H. Steyskal, "Simple method for pattern nulling by phase perturbation," *IEEE Transactions on Antennas and Propagation*, vol. 31, no. 1, pp. 163–166, Jan 1983.

[12] L. Poli, P. Rocca, G. Oliveri, and A. Massa, "Adaptive nulling in time-modulated linear arrays with minimum power losses," *IET Microwaves, Antennas Propagation*, vol. 5, no. 2, pp. 157–166, Jan 2011.

[13] P. Rocca, L. Poli, G. Oliveri, and A. Massa, "Adaptive nulling in time-varying scenarios through time-modulated linear arrays," *IEEE Antennas and Wireless Propagation Letters*, vol. 11, pp. 101–104, 2012.

[14] W. Kummer, A. Villeneuve, T. Fong, and F. Terrio, "Ultra-low sidelobes from time-modulated arrays," *IEEE Transactions on Antennas and Propagation*, vol. 11, no. 6, pp. 633–639, 1963.

[15] C. He, A. Cao, X. Liang, R. Jin, and J. Geng, "Beamforming method with periodical amplitude modulation array," in *2013 IEEE Antennas and Propagation Society International Symposium (APSURSI)*, July 2013, pp. 874–875.

[16] R. W. Heath, N. González-Prelcic, S. Rangan, W. Roh, and A. M. Sayeed, "An overview of signal processing techniques for millimeter wave mimo systems," *IEEE Journal of Selected Topics in Signal Processing*, vol. 10, no. 3, pp. 436–453, April 2016.

[17] J. Chen, X. Liang, R. Jin, J. Geng, C. He, and P. Li, "Efficiency improvement for time modulated antenna arrays," in *Accepted for publication in Proc. of 2016 IEEE International Symposium on Antennas and Propagation and USNC-URSI Radio Science Meeting (2016 IEEE AP-S & USNC-URSI)*, Fajardo, Puerto Rico, Jun. 2016.

Roberto Maneiro-Catoira received the Telecommunications Engineering degree from the University of Vigo, Spain, in 1995 and the Master of Information and Telecommunications Technologies for Mobile Networks degree in 2012 from the University of A Coruña, Spain, in 2012. He worked from 1996 to 1997 at Egatel company focused on the Research and Development in the field of TV and Radio digital communications. From 1997 to 2000 he was with Siemens Mobile Networks as GSM access network deployment manager. From 2000 to 2003 he worked at Nortel Networks as UMTS network integration manager. From 2003 he is fully dedicated to teaching Siemens Simatic Programmable Logic Devices as well as mathematics for different levels, both for private and public organisms. Actually he is working towards his Ph.D. about dynamic arrays for digital communications in the Electronic Technology and Communications Group (GTEC) at the University of A Coruña.

Julio C. Brégains received in 2000 the B.S. in Electrical Engineering from the National University of the Northeast, Argentina, and the Industrial Engineering degree from the University of León, Spain, in 2006. In 2007 he obtained with honors a Ph.D. degree in Applied Physics from the University of Santiago de Compostela (USC), Spain. He is currently an Assistant Professor of Electronics at the Department of Electronics and Systems of the School of Informatics, at the University of A Coruña, Spain. He is also currently a member of the Electronic Technology and Communications Group (GTEC), at that department. He has co-authored over 80 international journal and conference papers, having received awards for three of them. His research interests include high-frequency electronics, software development for solving electromagnetic problems, antenna array pattern synthesis and design, and variational problems applied to field theory.

José A. García-Naya studied Computer Engineering at the University of A Coruña (UDC), Spain, where he obtained his M.Sc. degree in 2005, and his Ph.D. degree with the distinction "Doctor with European Mention" in 2010. Since 2005 he is with the Group of Electronics Technology and Communications (GTEC) at the UDC, where he is currently Associate Professor. José A. García-Naya is coauthor of more than seventy papers in peer-reviewed international journals and conferences. He has also been member of the research team in more than forty research projects funded by public organizations and private companies. His research interests are in the field of wireless communication systems, with special emphasis on their experimental evaluation.

Luis Castedo was born in Santiago de Compostela, Spain, in 1966. He received the Ingeniero de Telecomunicación and Doctor Ingeniero de Telecomunicación degrees, both from Polytechnic University of Madrid, Spain, in 1990 and 1993, respectively. From November 1994 to October 2001, he was an Associate professor in the Department of Electronics and Systems at University of A Coruña, Spain, where he is currently Full Professor. He has been chairman of the Department between 2003 and 2009. Luis Castedo is coauthor of more than one hundred papers in peer-reviewed international journals and conferences. He has also been principal researcher in more than thirty research projects funded by public organizations and private companies. His research interests are signal processing and digital communications with special emphasis on blind adaptive filtering, estimation/equalization of MIMO channels, space-time coding and prototyping of digital communication equipments.